Article

A Simplified Silty Sand Model

Nopanom Kaewhanam and Krit Chaimoon *

Posted Date: 31 May 2023

doi: 10.20944/preprints202305.2232.v1

Keywords: clean sand; silty sand; elastoplastic model; critical state model; critical state line; simple model; three-dimensional stress

Article

A Simplified Silty Sand Model

Nopanom Kaewhanam [1] and Krit Chaimoon [2,*]

[1] Department of Civil Engineering, Faculty of Engineering, Mahasarakham University, Maha Sarakham 44150, Thailand; nopanom.k@msu.ac.th
[2] Department of Civil Engineering, Faculty of Engineering, Mahasarakham University, Maha Sarakham 44150, Thailand; k.chaimoon@msu.ac.th
* Correspondence: k.chaimoon@msu.ac.th

Abstract: A unified critical state model has been developed for both clean sand and silty sand using the modified Cam-clay model (MCC). The main feature of the proposed model is a new critical state line equation in the e-ln(p) plane that is capable of handling both straight and curved test results. With this feature, the error in calculating plastic volumetric strain is eliminated in theory. Another crucial feature of the model is the transformed stress tensor based on the SMP (spatially mobilized plane) criterion, which takes into account the proper shear yield and failure of soil under three-dimensional stresses. Additionally, the proposed model applies the intergranular void ratio with the fines influence factor for silty sand. Only eight soil parameters are required for clean sand, and a total number of twelve soil parameters are needed for silty sand.

Keywords: clean sand; silty sand; elastoplastic model; critical state model; critical state line; simple model; three-dimensional stress

1. Introduction

The modified Cam-clay (MCC) model was originally developed to describe the stress-strain-strength characteristics of normally-consolidated clay based on Roscoe and Burland's critical state theory [1]. A number of modifications have been made to the MCC to improve its ability to model geomaterials, such as [2–13]. Within the MCC and its family, the critical state void ratio (e_{cs}) defined by the critical state line (CSL) is assumed to be a straight line lower than the normally consolidated line (NCL) with the same slope λ, as shown in Figure 1(a). The distance between the NCL and CSL is assumed to be $(\lambda - \kappa)\ln(2)$. Eq. (1) contains two fitting parameters: Γ, the limiting critical state void ratio, usually defined as e_{cs} at p =1.0, and λ, which represents the constant slope of the CSL. However, unlike clay, the literature shows that the CSL of granular soil is not a straight line, e.g., [14–20]. A power function curve shown in eq. (2) provides a better representation for granular soil. In eq. (2), Γ acts as the upper bound of e_{cs}, while λ, p_a *and* ξ are the fitting parameters. Although p_a is recommended, it is not necessary to be the atmospheric pressure (approximately 101 kPa). Thus, eq. (2) requires three fitting parameters. It should be noted that the slope of CSL in eq. (2) is not a constant but a varied value $\bar{\lambda}$. A comparison between eq. (1) and eq. (2) is demonstrated in Figure 1(b). Using eq. (1) for granular soil would result in a significant error in the volumetric plastic strain ($\Delta\varepsilon_v^p = \Delta e^p/(1+e_0)$). Therefore, a power function curve is popularly used for sand or silty sand. However, this form of the power function can be problematic in sand models when dealing with high pressure because it cannot provide a straight portion after the curved portion. Figure 2(a) shows the concavity on the extension of eq. (2) after fitting the laboratory data [2], where the dashed line deviated from the trend of a straight line. To achieve a proper function of e_{cs} in the e-ln(p) for granular soil, including clean sand and silty sand, without any error in the volumetric plastic strain calculation, a curve illustrated in Figure 2(b) is required.

$$e_{cs} = \Gamma - \lambda \ln(p) \tag{1}$$

$$e_{cs} = \Gamma - \lambda\left(p/p_{ref}\right)^{\xi} \tag{2}$$

Preprints.org (www.preprints.org) | NOT PEER-REVIEWED | Posted: 31 May 2023 doi:10.20944/preprints202305.2232.v1

Matsuoka et al. [4] were the first to revise the shear yield and shear failure in the MCC model from the extended Mises criterion to the SMP criterion by introducing the transformed stress. Yao et al. [5] successfully applied the transformed stress of [4] to model loose and dense sand, depending on two key factors, i.e., the initial density (e_0) and mean effective stress (p_0). Furthermore, Yao et al. [6] proposed another transformed stress, in conjunction with a new hardening parameter, to the MCC model to model both clay and sand. Finally, in this study, a new curve of the CSL in the e-ln(p) is derived, which has the ability to fit a straight line, curved line, and a curved line connected with a straight line. Therefore, the sand model developed by Yao et al. [5] can be extended for both clean sand and silty sand. Additionally, we have made some revisions to the work of Yao et al. [5] to take into account the effect of the participation of fines in sand by applying the concept of the equivalent intergranular void ratio (e^*) proposed by Thevanayagam and Martin [21] and the fines influence factor (β) proposed by Lashkali [22]. The roundness of both sand and fines can settle the arguments in the load bearing mechanism of many silty sands in the literature, according to the work of Lashkali [22]. With these ideas, it is possible to oversimplify the soil characteristics in the critical state model for silty sand.

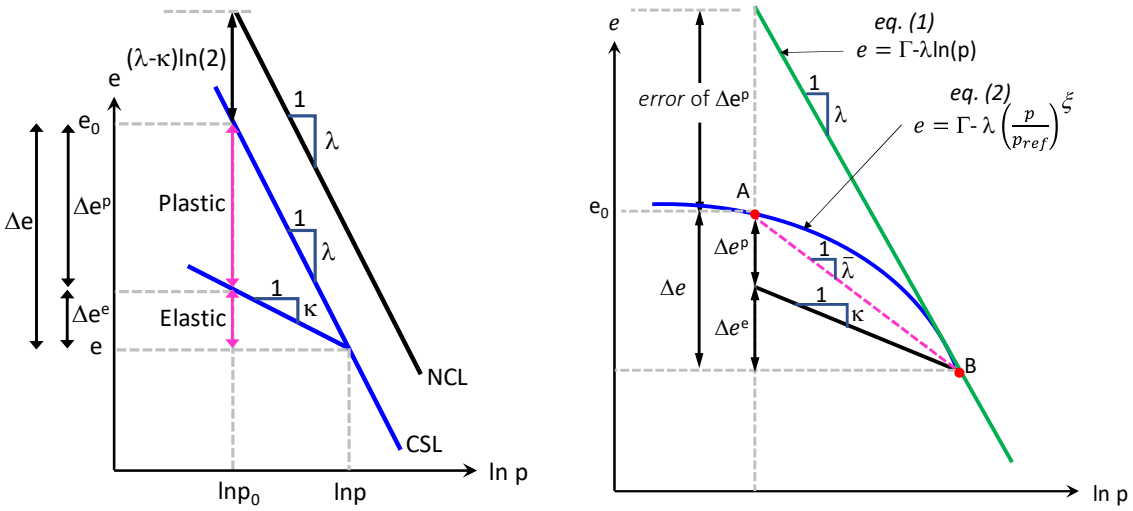

(**a**) (**b**)

Figure 1. Critical state line (CSL): (**a**) Normally consolidation line (NCL) and critical state line in MCC and MCC's family; (**b**) Comparison between CSL in eq. (1) and eq. (2).

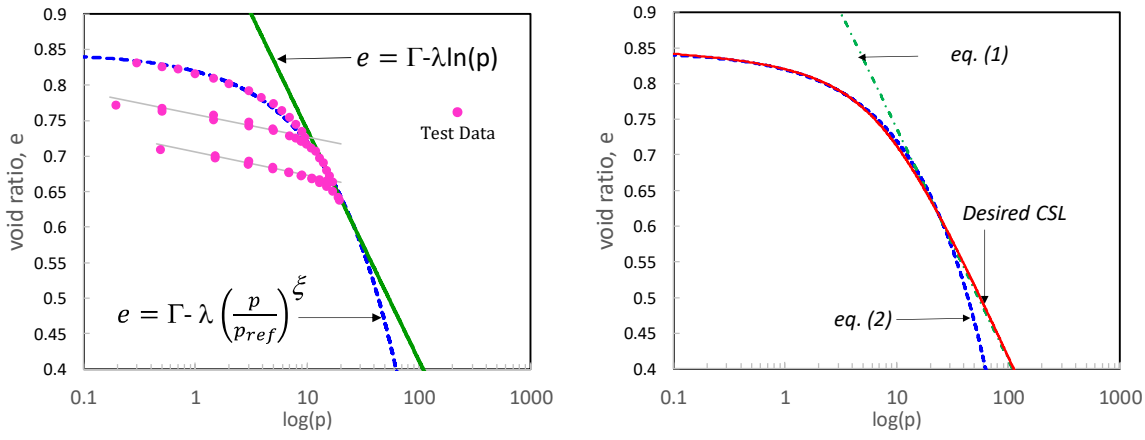

(**a**) (**b**)

Preprints.org (www.preprints.org) | NOT PEER-REVIEWED | Posted: 31 May 2023 doi:10.20944/preprints202305.2232.v1

Figure 2. Comparison of critical state lines: (**a**) Test data [2] vs eq. (1) and eq. (2); (**b**) required CSL vs eq. (1) & eq. (2).

2. The Critical State Line in e-ln(p) plane

As mentioned earlier, the MCC model adopted a straight line of the CSL, but a curved line is valid for sand and silty sand. To address this, the proposed CSL should have the following features:

1) The equation should provide both the curved portion and the connecting straight line
2) One of the fitting parameters should be the desired slope of the straight portion
3) The equation should consist of the parameters that can adjust to fit various curvatures and locations
4) All parameters should be determined from a conventional test

By incorporating these features, the proposed CSL can better capture the behavior of sand and silty sand, and provide more accurate predictions for engineering analyses.

Eq. (3) presents the new CSL with four fitting parameters: Γ, which controls the vertical translation of the curve; p_{ref}, which is a positive reference pressure controlling the horizontal translation; θ, which controls the curvature of the upper portion; and α, which controls the slope of the lower portion. It is recommended that the value of $\alpha = \lambda/2$ or a value close to $\lambda/2$, where λ is the slope of CSL in eq. (1). To investigate eq. (3), variations of all fitting parameters were demonstrated in Figures 3–6. Notably, when $\theta = 0$, the curvature of the CSL vanishes and eq. (3) becomes a straight line with a slope of 2α, as shown in eq. (4). Furthermore, when $\theta = 0$ and $p_{ref} = 1$, eq. (3) reduces to eq. (1) with $\alpha = \lambda/2$. Figure 7, the test results of Toyoura sand [2] were plotted against eq. (1), eq. (2) and eq. (3) to evaluate their performance. Eq. (5) and eq. (6) present the slope $\bar{\lambda}$ of eq. (3) in terms of tangential and secant, respectively.

$$e = \Gamma - \alpha \ln\left(\frac{p}{p_{ref}}\right) - \sqrt{\theta + \left(\alpha \ln\left(\frac{p}{p_{ref}}\right)\right)^2} \tag{3}$$

$$e = \Gamma - 2\alpha \ln\left(\frac{p}{p_{ref}}\right) \tag{4}$$

While eq. (3) requires more parameters than eq. (1-2), all four parameters can be determined by fitting the same test data used for eq. (1-2), without requiring additional testing. Therefore, eq. (3) satisfies all the aforementioned features.

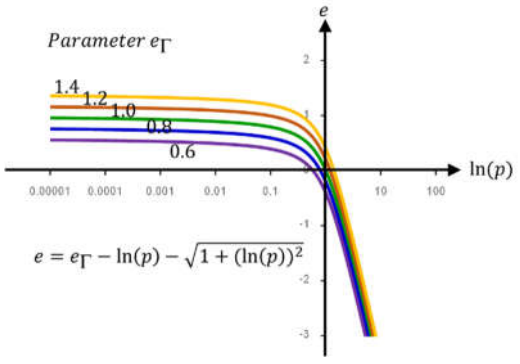

Figure 3. Effects of parameter Γ in eq. (3) for $0.6 \leq \Gamma \leq 1.2$.

Preprints.org (www.preprints.org) | NOT PEER-REVIEWED | Posted: 31 May 2023 doi:10.20944/preprints202305.2232.v1

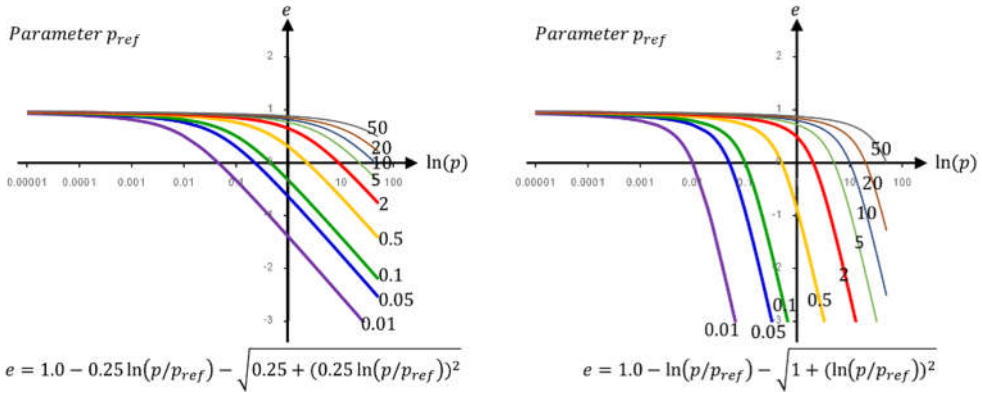

(**a**) (**b**)

Figure 4. Effect of parameter p_{ref} of eq. (3) when e_I=1.0: (**a**) α=θ= 0.25; (**b**) α=θ= 1.0.

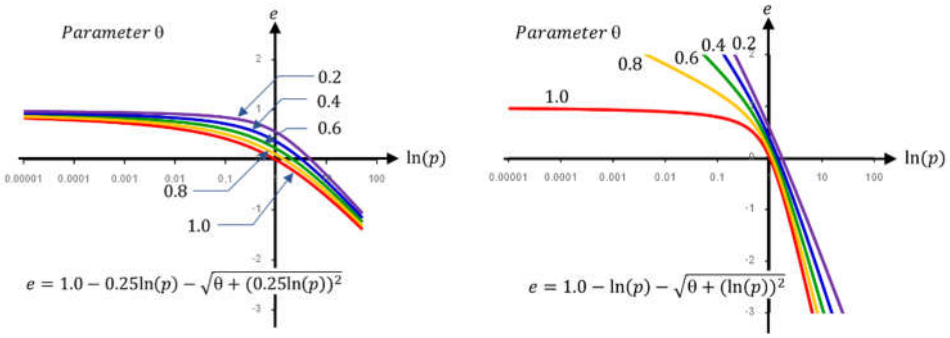

(**a**) (**b**)

Figure 5. Effect of parameter θ of eq. (3) when e_I=1.0: (**a**) at low value α= 0.25; (**b**) at high value α= 1.0.

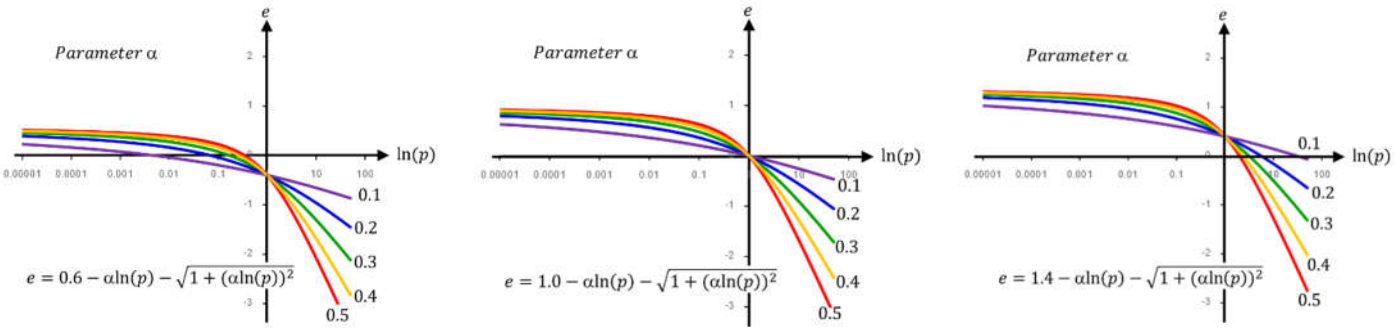

(**a**) (**b**) (**c**)

Figure 6. Effect of parameter α for e-p in equation (3) for θ=1.0: (**a**) e_I = 0.6; (**b**) e_I = 1.0; (**c**) e_I = 1.4.

Preprints.org (www.preprints.org) | NOT PEER-REVIEWED | Posted: 31 May 2023 doi:10.20944/preprints202305.2232.v1

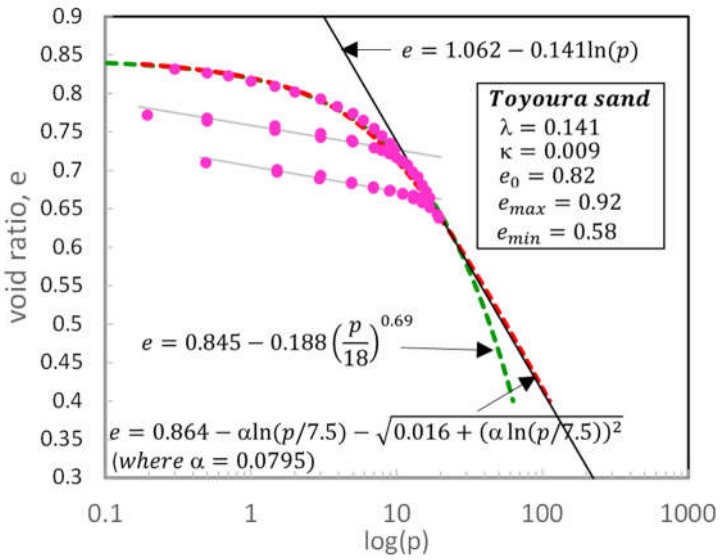

Figure 7. Evaluation of eq. (1), eq. (2) and (3) for Toyoura sand (experimental data from [2]).

$$\bar{\lambda}_t = \frac{\partial e}{\partial(lnp)} = \alpha\left[1 + \frac{\alpha\ln\left(\frac{p}{p_{ref}}\right)}{\sqrt{\theta + \left(\alpha\ln\left(\frac{p}{p_{ref}}\right)\right)^2}}\right] \tag{5}$$

$$\bar{\lambda}_s = -\frac{\Delta e}{\Delta\, ln(p)} = = \alpha + \left\{\sqrt{\theta + \left(\alpha\, ln\left(\frac{p_1}{p_{ref}}\right)\right)^2} - \sqrt{\theta + \left(\alpha\, ln\left(\frac{p_2}{p_{ref}}\right)\right)^2}\right\} / ln\left(\frac{p_2}{p_1}\right) \tag{6}$$

In the MCC model and its family, the CSL and NCL are both assumed to be a straight line with a constant slope λ (see Figure 1) and the vertical distance of $(\lambda - \kappa)\ln(2)$ [5]. In the proposed model, once the curve of NCL is obtained using eq. (3), the CSL is assumed to locate below the NCL with a distance of $\langle\bar{\lambda} - \kappa\rangle\ln(2)$, where $<>$ represents the Macualey brackets (i.e., $\bar{\lambda} - \kappa = \bar{\lambda} - \kappa$ when $\bar{\lambda} - \kappa \geq 0$ and zero otherwise). The shape and location of NCL compared to the CSL for this case are shown in Figure 8 (a). It is evident that both the CSL and NCL contain both curved and straight portions. Within the curve portion, the NCL and CSL have different slopes, and these lines are close together when the mean effective stress converges to a very small value ($p \to 0$). On the other hand, the CSL is parallel to the NCL with the same slope within the straight portion. This implies that the new CSL is not only applicable for granular soil but also for clay in the MCC model.

In addition, a curved of RCL can also be derived from the CSL by assuming that the shape of the CSL and the RCL are identical. Therefore, both CSL and RCL have the same parameters i.e., Γ, α and θ. The remaining parameter of the RCL is p_{ref} which can be determined by the horizontal translation of the CSL to the right until the vertical distance between the two straight portions of the CSL and RCL is equal to $\langle\bar{\lambda} - \kappa\rangle\ln(2) \approx \langle 2\alpha - \kappa\rangle\ln(2)$. Since the straight portions are parallel with the slope of 2α, then the horizontal distance between two straight lines is $(2\alpha - \kappa)\ln(2)/(2\alpha)$. Hence, the parameter $p_{ref(RCL)} = p_{ref(CSL)} * 2\text{^}((2\alpha - \kappa)/(2\alpha))$.

Preprints.org (www.preprints.org) | NOT PEER-REVIEWED | Posted: 31 May 2023 doi:10.20944/preprints202305.2232.v1

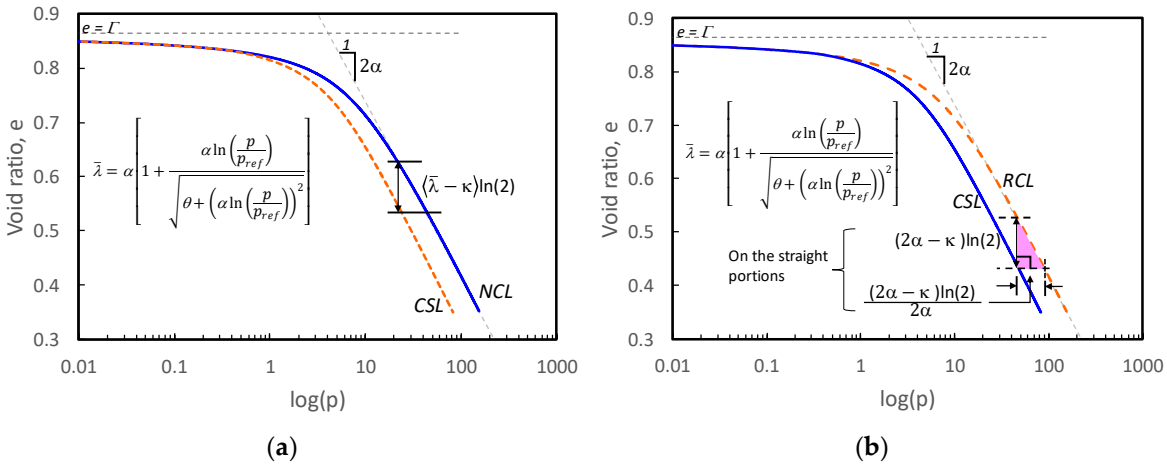

(**a**) (**b**)

Figure 8. Shape and location of the CSL compared to the RCL in the proposed model using the tangential slope $\bar{\lambda}$ in eq. (5): (**a**) CSL is derived from the NCL; (**b**) RCL is derived from the CSL.

3. Critical State Model for Clean Sand

In the work of Yao et al. [5], the NCL was used as a key tool to distinguish between loose and dense sand, using as a reference control line (RCL). Therefore, in this case, the terms loose and dense refer to sands that are looser or denser than the RCL. Due to changes in the RCL and CSL, some revisions were required to the model presented in [5]. Before describing the revisions in detail, a clearly summary of sand behavior for both loose and dense conditions is stated as follows:

1) Sand on RCL exhibits only volume contraction during shearing, and the stress ratio $\eta = q/p$ reaches its maximum value at the critical state, where $\eta = M_c$ and M_c is the slope of the critical state line on p-q plane.
2) Sand that is looser than the RCL (sheared from a point above the RCL) exhibits only volume contraction, but with the larger amount than sand on the RCL and finally reaches the same maximum stress ratio as sand on the RCL at $\eta = M_c$.
3) Sand that is denser than the RCL (sheared from a point below the RCL) exhibits volume contraction in early stage, followed by dilation (the stress ratio is greater than the maximum stress ratio of sand on the RCL, i.e., $(\eta = M_f) > M_c$, and finally converges to the stress ratio $\eta = M_c$.

It is evident that both sand on RCL and sand looser than RCL have no peak, but reach the same maximum stress ratio at the critical state, while a peak exists in dense sand during shearing before reaching the critical state. Figure 9 depicts the concept mentioned above.

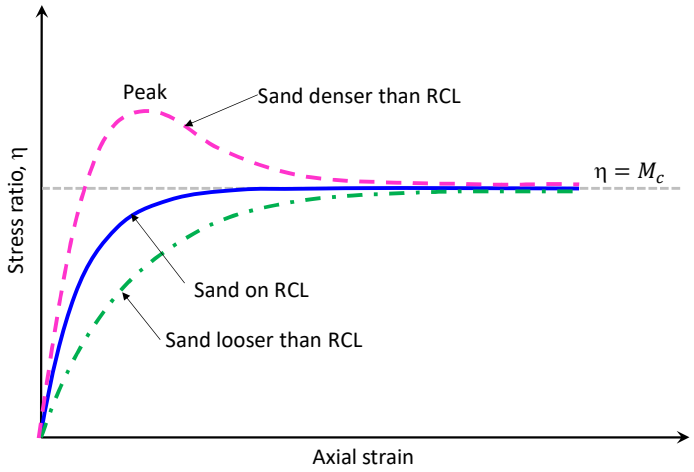

Figure 9. Schematic drained stress-strain curves of sand at different initial state.

 doi:10.20944/preprints202305.2232.v1

3.1. Hardening parameter H

The equation for the hardening parameter H in the MCC model and in Yao et al. [5] are shown in eq. (7) and eq. (8), respectively. In eq. (7), λ is a constant representing the slope of the straight NCL and a variable c_p is defined as $c_p = (\lambda\text{-}\kappa)/(1+e_0)$. In eq. (8), despite using the straight NCL in [5], the varied slope of the NCL $\bar{\lambda}$ is assumed in such a way that $\bar{c}_p = (\bar{\lambda}\text{-}\kappa)/(1+e_0) = [(\lambda\text{-}\kappa)/(1+e_0)](Mc/Mf)$, where *Mc* and *Mf* are the stress ratio at the critical state and stress ratio during shearing. As mentioned in the early section, loose sand has no peak, so *Mf* = *Mc*, resulting in eq. (8) becomes eq. (7) of the MCC model. On the other hand, for dense sand, *Mf* ≥ *Mc* during shearing. In this paper, a new value of $\bar{\lambda}$ can be calculated directly from the RCS without any assumption using the secant slope of the RCL in eq. (6). Therefore, the final version of H in the proposed model is shown in eq. (9).

$$H = \int dH = \int \frac{1}{c_p} d\varepsilon_v^p \; ; (c_p = \frac{\lambda - \kappa}{1 + e_0}) \tag{7}$$

$$H = \int dH = \int \frac{1}{\bar{c}_p} \frac{M_c^4}{M_f^4} \frac{M_f^4 - \eta^{*4}}{M_c^4 - \eta^{*4}} d\varepsilon_v^p \; ; (\bar{c}_p = \frac{\bar{\lambda} - \kappa}{1+e_0} = \frac{\lambda - \kappa}{1+e_0} \frac{M_c^4}{M_f^4}) \tag{8}$$

where η^* is the maximum stress ratio during shearing.

$$H = \int dH = \int \frac{1}{\bar{c}_p} \frac{M_f^4 - \eta^{*4}}{M_c^4 - \eta^{*4}} d\varepsilon_v^p \; ; (\bar{c}_p = \frac{\bar{\lambda} - \kappa}{1 + e_0} \; ; \; \bar{\lambda} \; calculated \; by \; eq. (6)) \tag{9}$$

3.2. Yield function

The yield function of the MCC model is represented by an ellipse in p-q plane, as shown in eq. (10). To account for the behavior of loose sand, Yao et al. [5] introduced the initial state parameter χ ($0 \leq \chi \leq 1$) into the MCC model, resulting in a Lemniscate-shaped yield function [23] as shown in eq. (11). The value of χ is zero when sand is on the RCL, and χ increases with distance above the RCL i.e., χ links to both the shape of the yield function and the distance above the RCL. Hence, χ can describe the degree of looseness of sand. Figure 10 (a) shows the yield functions of eq. (10) and eq. (11).

$$f = ln\left(\frac{p}{p_0}\right) + ln(1 + \eta^2/M^2) = \int dH \tag{10}$$

$$f = \ln\left(\frac{p}{p_0}\right) + \ln\left(1 + \frac{\eta^2/M^2}{1 - \chi\eta^2/M^2}\right) = \int dH \tag{11}$$

According to [5], the original value of χ is derived by the stress path of a constant mean effective stress (p′ = p′0) as expressed in eq. (12). The modified χ by incorporating the yield function in eq. (11) and the new hardening in eq. (9) by the same method of [5] is shown in eq. (13).

$$\chi = \frac{EXP\left(\frac{e_0 - e_{cs@p0}}{\lambda - \kappa}\right) - 2}{EXP\left(\frac{e_0 - e_{cs@p0}}{\lambda - \kappa}\right)} \; ; \chi \geq 0 \tag{12}$$

$$\chi = \frac{EXP\left(\frac{e_0 - e_{cs@p0}}{\bar{\lambda}_0 - \kappa}\right) - 2}{EXP\left(\frac{e_0 - e_{cs@p0}}{\bar{\lambda}_0 - \kappa}\right)} \; ; \chi \geq 0 \tag{13}$$

where $e_{cs@p0}$ is the critical void ratio calculated by eq. (3) at the initial mean stress p_0. In eq. (13) $\bar{\lambda}_0$ is calculated using the tangential slope of the RCL in eq. (5) at the initial mean effective stress p_0.

The state parameter χ in eq. (13) is constant during shearing and depends on both the initial mean effective stress p0 and the initial void ratio e0. For sand on the RCL, the $\bar{\lambda}_t$ and $\bar{\lambda}_s$ in eq. (5-6), respectively, are applicable. For loose sand, the e0 is located above the RCL, the $\bar{\lambda}_t$ can be assumed by the interpolation function as shown in eq. (14). Figure 10 illustrates the effect of the initial parameter χ to the yield function and stress-strain curves from the drained triaxial compression simulation. Figure 11 shows the comparison between the test results and the predictions from the

Preprints.org (www.preprints.org) | NOT PEER-REVIEWED | Posted: 31 May 2023 doi:10.20944/preprints202305.2232.v1

MCC, Sand model by Yao et al. [5] and the proposed model. In the analyses, seven soil parameters for loose sand are listed in Table 1 [2].

$$\bar{\lambda}_t = \bar{\lambda}_{(RCL)} + \chi(2\alpha - \bar{\lambda}_{(RCL)}) \quad (14)$$

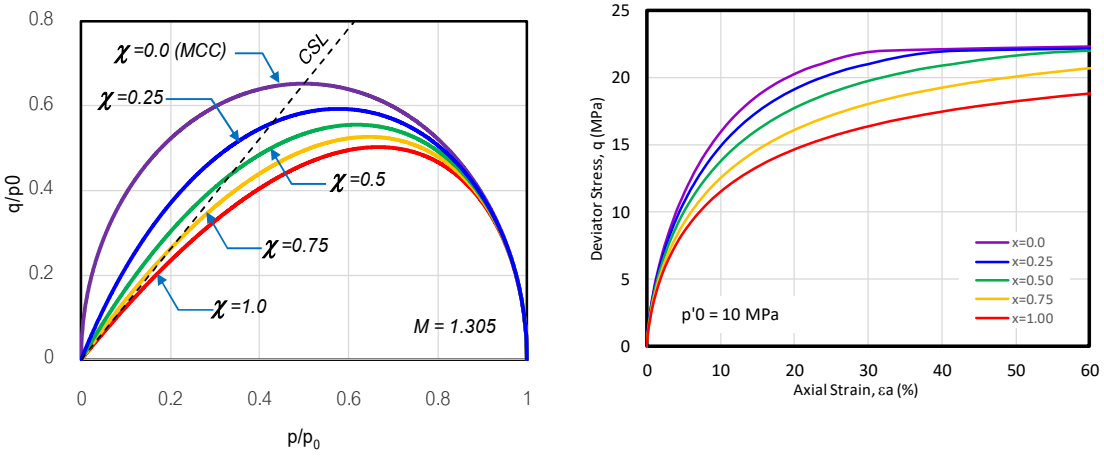

(**a**) (**b**)

Figure 10. Effect of parameter χ to the MCC model: (**a**) yield function of the MCC (eq. (7) vs yield function of loosed sands eq. (8) (χ = 0 to 1); (**b**) stress-strain curves for loose sands from drained triaxial compression simulation using both parameter χ and $\bar{\lambda}$.

Table 1. Soil parameters for drained analyses.

Soil Model	Γ	α	θ	p_{ref}	λ	κ	M_c	ν
MCC and Sand Model [5]	1.97	-	-	-	0.141	0.009	1.305	0.3
Proposed Model	0.864 *	0.0795 *	0.016 *	7.5 *	-	0.009	1.305	0.3

* Fitting parameters from existing data of the NCL (see Figure 7).

In Figure 11, the predictions from both the MCC model and sand model by Yao at al. [5] overestimate the shear strength of sand. However, the results from [5] provides a better result than the MCC's because of the improvement of the plastic strain calculation through the parameter χ. For the proposed model with both the initial parameters χ and $\bar{\lambda}$, the prediction agrees well with test results.

Preprints.org (www.preprints.org) | NOT PEER-REVIEWED | Posted: 31 May 2023 doi:10.20944/preprints202305.2232.v1

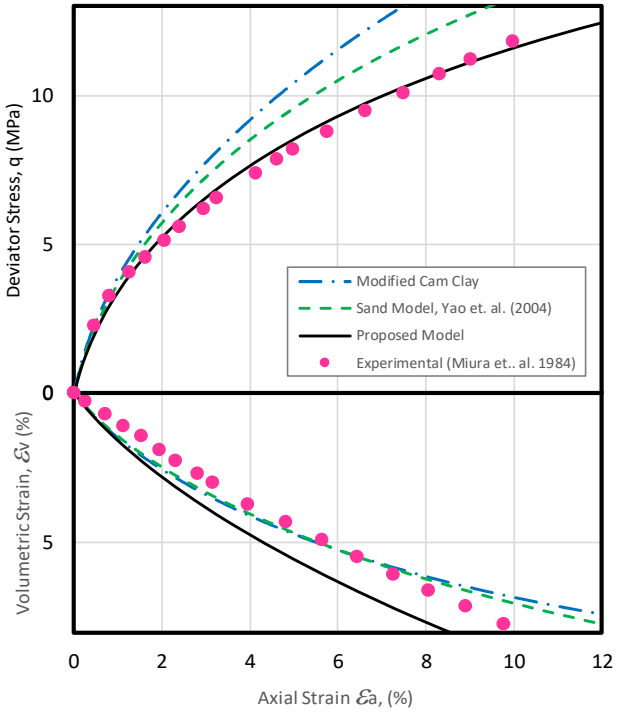

Figure 11. Comparison of the predictions from the MCC model, sand model [5] and the proposed model to the test data [2].

3.3. Peak strength of dense sand

In [5], the yield function of the MCC model can be used for dense sand without the modifications i.e., $\chi = 0$ in eq. (11-12). The goal then becomes identifying the peak in the stress-strain relationship of dense sand. A beautiful derivation for another state parameter χ_2 controlling M_f during shearing is introduced to the MCC model in Yao et al. [5] as shown in eq. (15). The additional soil parameter M_{fmax} and Nd are required to work with its state parameter. Although this formulation works, it required the densest condition for sand in the calculation. Furthermore, Yao et al. [5] assumed the slope of the densest condition to be the same value of the slope of the unloading-reloading curve with a constant slope κ. The computation for M_f is required to be changed in order to simplify the model for sand and silty sand.

Been and Jeffries [24] introduced the effective state parameter for sand $\psi = e - e_{cs}$ where e and e_{cs} are the void ratio and the critical state void ratio at the same mean effective stress, respectively. In [25,26], the relationships of M_f are proposed relating to $\psi = e - e_{cs}$. Some researchers have hypothesized that the ratio e/e_{cs} could function as a state parameter e.g., [27]. However, other researchers such as [28,29] favor using the mean effective stresses ratio p/p_{cs} where p and p_{cs} are the current and critical state mean effective stress. According to a comprehensive review by Lashkari [30], two of the most effective state variables which can provide a reasonable peak strength M_f of granular soil are $\Omega = I_D \ln(p_{cs}/p)$ and $\psi = e - e_{cs}$, where $I_D = (e_{max} - e)/(e_{max} - e_{min})$ is the relative density, e_{max} the maximum void ratio and e_{min} the minimum void ratio. The expression for M_f from Ω and ψ are shown in eq. (16) and eq. (17), respectively. In this research, we utilized the equation of Manzari and Dafalias [26] in eq. (17) in order to achieve the basic model without requiring many extra parameters.

$$M_f = M_{fmax}\sqrt{\chi_2} + M_c \tag{15}$$

$$M_f = M_c[1 + n_b I_D \ln(p_c/p)] \tag{16}$$

Preprints.org (www.preprints.org) | NOT PEER-REVIEWED | Posted: 31 May 2023 doi:10.20944/preprints202305.2232.v1

$$M_f = M_c[1 + n_b\langle -\psi \rangle] \quad (17)$$

Before moving forward to the next section of modeling silty sand, the predictive capability of clean sand for both loose and dense conditions are demonstrated by the comparison between the model prediction and two sets of the test results from Verdugo [31] and Verdugo and Ishihara [32]. Adding n_b to the model, eight soil parameters listed in Table 2 from [30–32] are used in the analyses for dense sand.

Table 2. Soil Parameters for undrained analyses.

Soil Parameter	Γ	α	θ	p_{ref}	κ	M_c	ν	n_b
Proposed Model	0.864 *	0.0795 *	0.004 *	3.06 *	0.02	1.265	0.25	1.34

* Fitting parameters from existing data of the CSL.

Figures 12 and 13 show the comparison of the test results and the calculation from the proposed model. In Figure 12, the results of the undrained triaxial tests at the initial mean effective stress of 490 kPa and three different initial void ratios of 0.861, 0.883, and 0.910 are demonstrated. Figures 12 (a) through (b) depict the test results, while Figures 12 (c) through (d) illustrate the results of calculation by the proposed model. The peak can be observed in the stress-strain curves of e0 = 0.883 and 0.910 on both the test results and the calculation. Figure 13 shows the results of the undrained triaxial tests for a fixed value of the initial void ratio e0= 0.833 and four different values of the initial mean effective stresses of 3,000, 2,000, 1,000 and 100 kPa. The peak occurred on the stress-strain curves of p0 = 3,000, 2,000, 1,000 kPa. The result demonstrates agreement between the peak from the calculation and the test. It is important to notice that when shearing reached the critical state, all stress-strain curves in Figure 13b,d tended to the same shear strength.

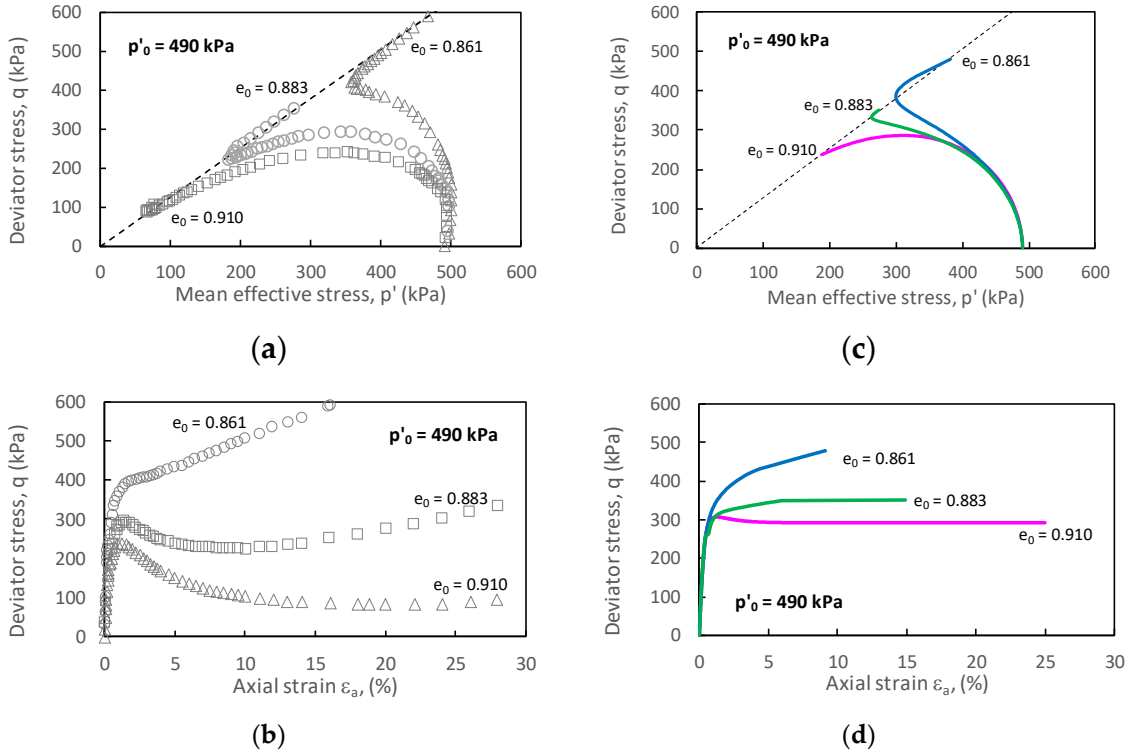

Figure 12. Undrained triaxial compression test results of clean sand at p0=490 kPa: (**a**) stress path (test results); (**b**) stress-strain curves (test results); (**c**) stress path (proposed model) (**d**) stress-strain curves (proposed model).

Preprints.org (www.preprints.org) | NOT PEER-REVIEWED | Posted: 31 May 2023 doi:10.20944/preprints202305.2232.v1

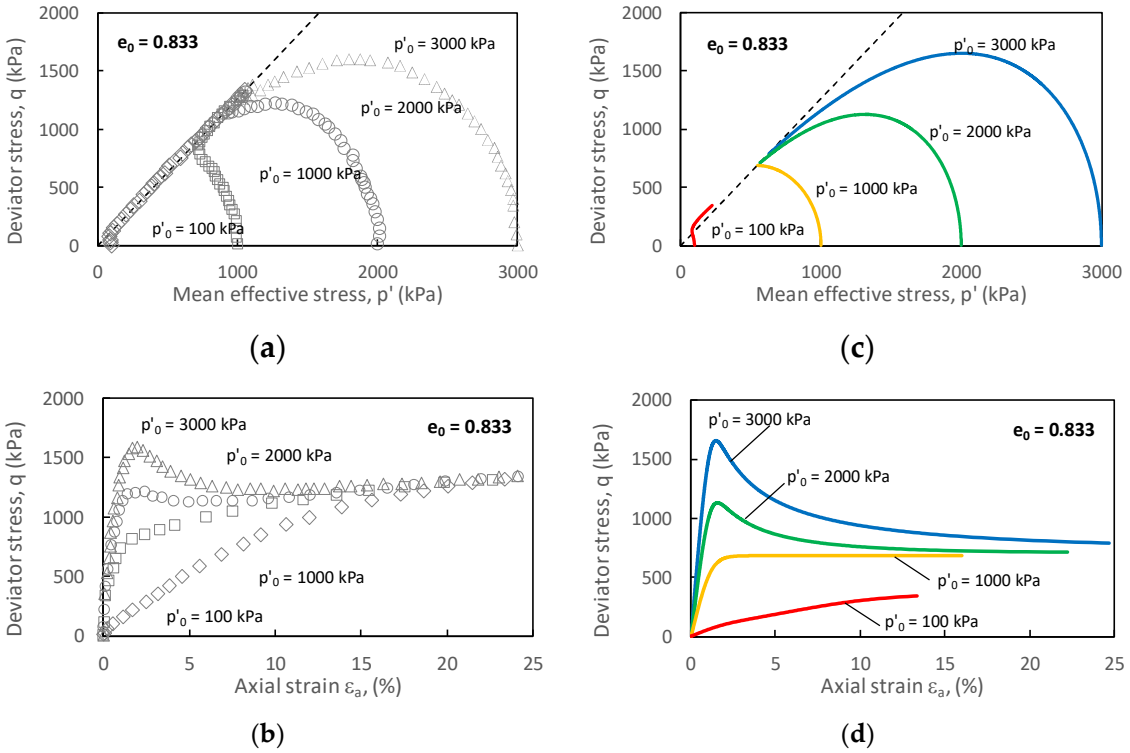

Figure 13. Undrained triaxial compression test results of clean sand at e0 = 0.833: (**a**) stress path (test results); (**b**) stress-strain curves (test results); (**c**) stress path (proposed model) (**d**) stress-strain curves (proposed model).

4. Critical State Model for silty sand

Due to the partial participation of fines in the void between sand grains. The equivalent intergranular void ratio (e*) suggested by Thevanayagam and Martin [21] was employed in place of the global void ratio to account for the effect of fines in sand. The equation of e* is expressed as follow

$$e^* = \frac{e + (1-\beta)FC}{1-(1-\beta)FC} \tag{18}$$

where β represents the fines influence factor and FC represents the amount of fines content. The reasonable value of β is $0 \ll \beta \ll 1$. When $\beta = 0$, $\beta = 1$ and $0 < \beta < 1$ fines take no action, fully action and partial action in the load bearing mechanism, respectively. The dependence of β on the particle size ratio SR = (d10 of host sand)/(d50 of silt) was discovered using experimental data from Ni et al. [33]. The empirical equation for β, presented by Lashkari [22], takes into account the impacts of the particle size ratio SR as well as the roundness of the soil grains as stated as follows

$$\beta = \beta_0 \times (FC) \times SR^{-0.2} \tag{19}$$

where

$$\beta_0 = (1.93 + 0.04\langle r-1\rangle^2)(1 + 3.2\langle r-1\rangle^2 EXP(-22FC)) \tag{20}$$

and r is the ratio of the average roundness of sand (rc) and fines (rf), respectively.

It is generally accepted that the CSL in the e-p space gradually moves downward when FC increases e.g., [18,34–39]. However, when drawing in terms of the equivalent intergranular void ratio e*, the CSL are close together in a narrow range. As a result, for different FC, a specific curve of the e*-p can be established. In this paper, the e* in eq. (18) is used to model the silty sand. Therefore, the state parameter for silty sand becomes $\psi^* = e^* - e_{cs}$ and the M_f for silty sand expressed as follow

$$M_f = M_c[1 + n_b\langle -\psi^*\rangle] \tag{21}$$

Preprints.org (www.preprints.org) | NOT PEER-REVIEWED | Posted: 31 May 2023 doi:10.20944/preprints202305.2232.v1

The amount of FC also affects the stress ratio at the critical state M_c. In the work of Lashkari [22], the value of M_c for the specific FC can be determined by the concept of threshold fines content (FC_{th}) expressed in eq. (22). The stress ratio at the critical state for FC ($M_c(FC)$) can be calculated by Lashkari [22] in eq. (23) with two more parameters i.e., $M_c(0)$ where the M_c at zero fines content and $\Delta M_c = M_c(FC_{th}) - M_c(0)$. The equations for the FC_{th} by Rahman [18], $M_c(FC)$ and by Lashkari [22] are presented in eq. (22-23).

$$FC_{th} = 0.4\left(\frac{1}{1+EXP(0.50-0.13\times SR)}+\frac{1}{SR}\right) \tag{22}$$

$$M_c(FC) = M_c(0) + \frac{3}{2}(\Delta M_c)\left(\frac{FC}{FC_{th}}\right)^2 - \frac{1}{2}(\Delta M_c)\left(\frac{FC}{FC_{th}}\right)^3 \tag{23}$$

As described above, five additional parameters are required in the analysis of silty sand i.e., rc, rf, SR, $M_c(0)$ and ΔM_c. Two sets of silty sand test results [18,39] are compared to the calculation of the proposed model as shown in Figures 14 and 15.

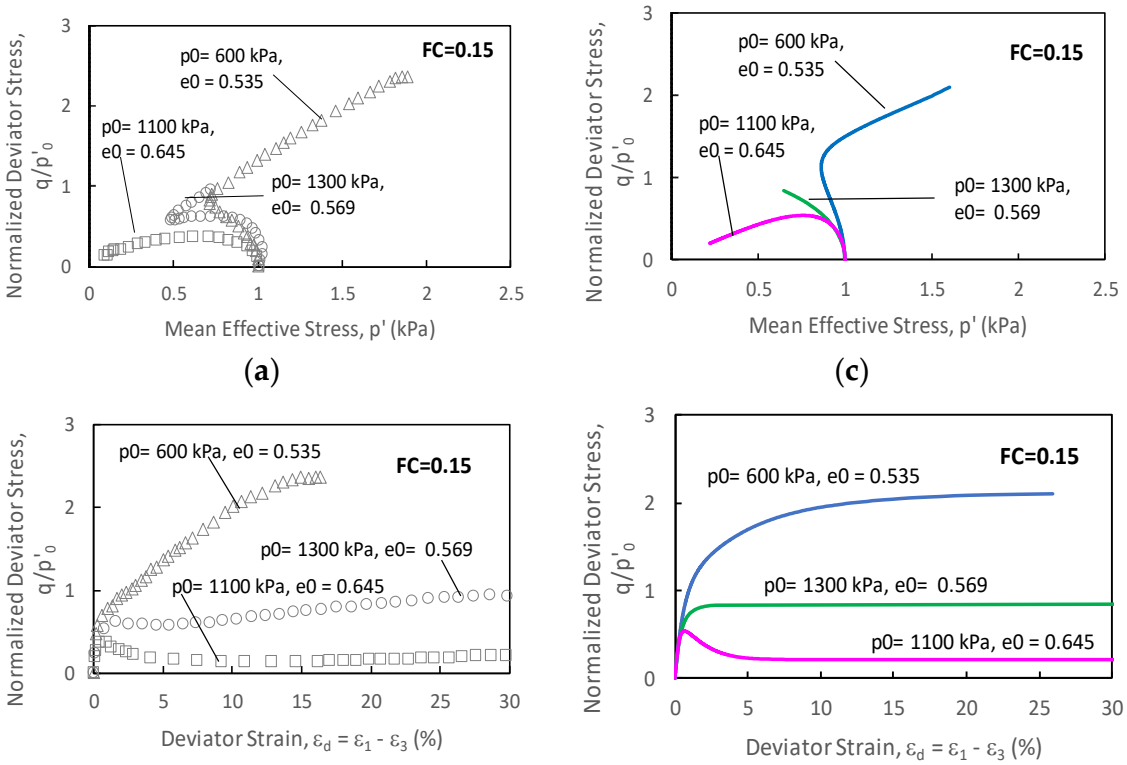

Figure 14. Undrained triaxial compression test results of silty sand for FC=0.15 (Rahman et al. [18]: (**a**) stress path (test results); (**b**) stress-strain curves (test results); (**c**) stress path (proposed model) (**d**) stress-strain curves (proposed model).

 doi:10.20944/preprints202305.2232.v1

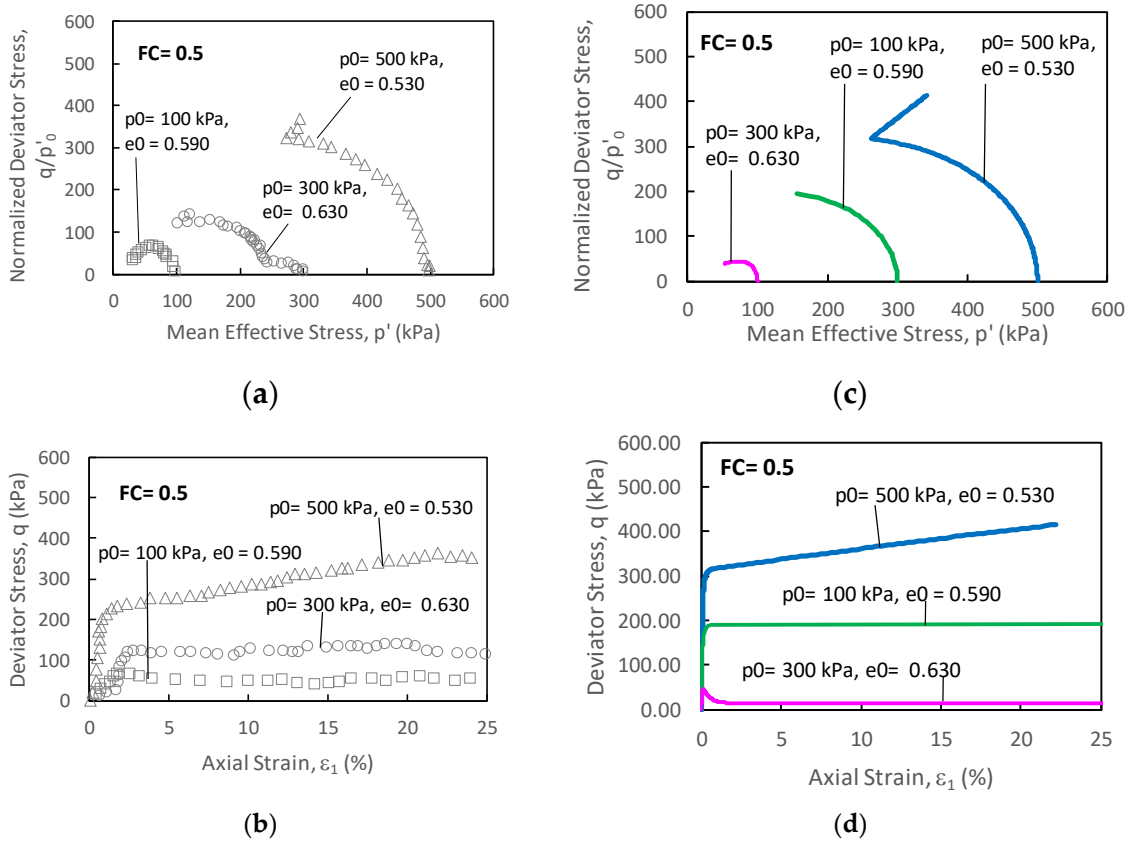

Figure 15. Undrained triaxial compression test results of silty sand for FC=0.50 (Huang et al. [39]: (**a**) stress path (test results); (**b**) stress-strain curves (test results); (**c**) stress path (proposed model) (**d**) stress-strain curves (proposed model).

5. Conclusions

Adding fines into voids of sand leads to a complex behavior of a whole silty sand. The degree of participation of fines in the load-bearing mechanism can be modeled using the intergranular void ratio e* and the fines influence factor β. Two key factors affecting the value of β are the particle size ratio SR and the roundness of soil grain (both sand and silt). To model the behavior of silty sand precisely, the critical state model has a rise in the complexity leading to twenty or more soil parameters. Therefore, most critical state for silty sand is not practical in general analysis especially for the limited budget project. Therefore, the simple silty sand model is needed. The modified Cam clay model (MCC) including the model in the MCC's family is considered as the simple critical state model in terms of the number of soil parameters. Much modification has been introduced to the MCC to improve its capability e.g., the SMP yield and failure criterion, effective hardening for both clay and sand, yield function for contractive soil. However, the MCC model and its family lack the link to the curve of the CSL which fits to behavior of granular soil. This paper introduces a new equation for the CSL which can be applied for the CSL in the straight-type, the curved type and the curve connecting by the straight portion. Four fitting parameters are used to control the shape and location of the CSL without extra testing. This feature not only improves the prediction for sand but also extends the capability of the model for silty sand in both drained and undrained analyses. Only eight parameters are required for clean sand (i.e., Γ, α, θ, p_{ref}, κ, ν, M_c and n_b). Five extra parameters are needed for silty sand i.e., rc, rf, SR, $M_c(0)$ and ΔM_c). It is worth to note that the M_c is no longer required for silty sand because M_c can be calculated from $M_c(0)$ and ΔM_c. Therefore, a total number of soil parameters for silty sand are twelve. The agreement between the prediction of the proposed model and the existing testing results from distinct researchers confirm that the proposed model is suitable for further analyses of both clean sand and silty sand.

 doi:10.20944/preprints202305.2232.v1

References

1. Roscoe, K. H.; Burland, J. B. On the generalized stress strain behavior of "wet" clay. *Engineering Plasticity*, **1968**, Cambridge Univ. Press., pp. 535–609.
2. Miura, Norihiko et al. "Stress-strain characteristics of sand in a particle-crushing region." Soils and Foundations 24 (1984): 77-89.
3. Wong, Tai T. et al. "A constitutive model for broken ice." Cold Regions Science and Technology 17 (1990): 241-252.
4. Matsuoka, H., Yao, Y. P.; Sun, D. A. The Cam-Clay Models Revised by the SMP Criterion. *Soils and Foundations*, **1999**, 39(1), pp. 81–95.
5. Yao, Y.P.; Sun, D.A.; Luo, T.A. Critical state model for sands dependent on stress and density. *International Journal for Numerical and Analytical Methods in Geomechanics*, **2004**, *28(4)*, pp. 323-337.
6. Yao, Y.P.; Sun, D.A.; Matsuoka, H. A unified constitutive model for both clay and sand with hardening parameter independent on stress path. *Computers and Geotechnics*, **2008**, *35(2)*, pp. 210-222.
7. Suebsuk, J.; Horpibulsuk, S.; Liu, M. D. A critical state model for overconsolidated structured clays. *Computers and Geotechnics*, **2011**, *38(5)*, pp. 648–658.
8. L. F. Cao, C. I. Teh, and M. F. Chang Undrained cavity expansion in modified Cam clay I: Theoretical analysis Volume 51 Issue 4, May 2001, pp. 323-334
9. Grimstad, Gustav et al. "Modeling creep and rate effects in structured anisotropic soft clays." Acta Geotechnica 5 (2010): 69-81.
10. Yin, Zhen-yu et al. "A simple critical-state-based double-yield-surface model for clay behavior under complex loading." Acta Geotechnica 8 (2013): 509-523.
11. Miranda, P.A.M.N. & Vargas, E.A. & Moraes, Anderson. (2019). Evaluation of the Modified Cam Clay model in basin and petroleum system modeling (BPSM) loading conditions. Marine and Petroleum Geology. 112. 104112. 10.1016/j.marpetgeo.2019.104112.
12. Miranda, P. A. M. N.; Vargas, E. A.; Moraes, A. Evaluation of the Modified Cam Clay model in basin and petroleum system modeling (BPSM) loading conditions. *Marine and Petroleum Geology*, **2020**, *112*, pp. 104-112.
13. Ou, Chang-Yu, C. C. Liu and C. K. Chin. "Anisotropic viscoplastic modeling of rate-dependent behavior of clay." International Journal for Numerical and Analytical Methods in Geomechanics 35 (2011): n. pag.
14. Li, X.S., Wang, Y., 1998. Linear representation of steady state line for sand. ASCE J. Geotech. Geoenviron. Eng. 124 (12), 1215–1217.
15. Yang, Z.X., Li, X.S., Yang, J., 2008. Quantifying and modelling fabric anisotropy of granular soils. Géotechnique 58 (4), 237–248.
16. Yang, Jun & Wei, L. & Dai, Beibing. (2015). State variables for silty sands: Global void ratio or skeleton void ratio?. Soils and Foundations. 55. 10.1016/j.sandf.2014.12.008.
17. Murthy, T. G., Loukidis, D., Carraro, J. A. H., Prezzi, M. & Salgado, R. (2007). Ge´otechnique 57, No. 3, 273–288
18. Rahman, M.M., Lo, S.R. & Baki, M.A.L. Equivalent granular state parameter and undrained behaviour of sand–fines mixtures. Acta Geotech. 6, 183–194 (2011).
19. Modelling the static liquefaction of sand with low-plasticity fines M.M. RAHMAN, S.-C.R. LO, and Y.F. DAFALIAS Géotechnique 2014 64:11, 881-894
20. J. Duriez, É. Vincens, Constitutive modelling of cohesionless soils and interfaces with various internal states: An elasto-plastic approach,Computers and Geotechnics,Volume 63,2015,Pages 33-45.
21. Thevanayagam S, Martin GR. Liquefaction in silty soils-screening and remediation issue. Soil Dyn Earthquake Eng 2002;22:1035–42.
22. Ali Lashkari, Recommendations for extension and re-calibration of an existing sand constitutive model taking into account varying non-plastic fines content, Soil Dynamics and Earthquake Engineering, Volumes 61–62, 2014, Pages 212-238.
23. Taiebat, Mahdi; Dafalias, Yannis F. (2010). Simple Yield Surface Expressions Appropriate for Soil Plasticity. International Journal of Geomechanics, 10(4), 161–169.
24. Been K, Jefferies MG. A state parameter for sands. Géotechnique 1985;35 (2):99–112.
25. Manzari MT, Dafalias YF. A critical state two surface plasticity model for sands. Géotechnique 1997;47(2):255–72.
26. Dafalias YF, Manzari MT. Simple plasticity sand model accounting for fabric change effects. ASCE J Eng Mech 2004;130(6):622–34.
27. Wan RG, Guo PJ. A simple constitutive model for granular soils: modified stress–dilatancy approach. Comput Geotech 1998;22(2):109–33.
28. Wang ZL, Dafalias YF, Li XS, Makdisi FI. State pressure index for modeling sand behavior. ASCE J Geotech Geoenviron Engng 2002;128(6):511–9.
29. Vesic A, Clough GW. Behavior of granular materials under high stresses. J Soil Mech Found Div ASCE 1968;94(SM3):661–88.

 doi:10.20944/preprints202305.2232.v1

30. Ali Lashkari, On the modeling of the state dependency of granular soils, Computers and Geotechnics, Volume 36, Issue 7,2009, 1237-1245
31. R. Verdugo. PhD dissertation. University of Tokyo (1992)
32. VERDUGO, RAMON; ISHIHARA, KENJI (1996). The Steady State of Sandy Soils.. SOILS AND FOUNDATIONS, 36(2), 81–91. doi:10.3208/sandf.36.2_81
33. Ni Q, Tan TS, Dasari GR, Hight DW. Contribution of fines to the compressive strength of mixed soils. Géotechnique 2004;54(9):561–9.
34. Stamatopoulos CA. An experimental study of the liquefaction strength of silty sands in terms of the state parameter. Soil Dyn Earthquake Eng 2010;30:662–78
35. Ventouras K, Coop MR. On the behavior of Thanet sand: an example of an uncemented natural sand. Géotechnique 2009;59(9):727–38.
36. Cubrinovski M, Rees S. Effects of fines on undrained behavior of sands. ASCE geotechnical publication no. 181 2008:1–11.
37. Rahman MM, Lo SR, Gnanendran CT. On equivalent granular void ratio and steady state behavior of loose sand with fines. Can Geotech J 2008;45:1439–56.
38. Papadopoulou A, Tika T. The effect of fines on critical state and liquefaction resistance characteristics of non-plastic silty sands. Soils Found 2008;48 (5):713–25.
39. Huang Y-T, Huang A-B, Kuo Y-C, Tsai M-D. A laboratory study on the undrained strength of silty sand from Central Western Taiwan. Soil Dyn Earthquake Eng 2004;24:733–43.